

Electronic Desymmetrization of $\text{Cu}_3(\mu_3\text{-E})$ Clusters (E = S, Se) Induced by Edge-to-Face π -Stacking Interactions in the Second Coordination Sphere

Pinar Alayoglu, M. Victoria Lorenzo Ocampo, Zhiyu Wang, Tiejian Chang, Yu-Sheng Chen, Mingjie Liu,* Leslie J. Murray,* and Neal P. Mankad*



Cite This: *Inorg. Chem.* 2024, 63, 24501–24505



Read Online

ACCESS |



Metrics & More



Article Recommendations



Supporting Information

ABSTRACT: A pair of cyclophane-encapsulated $[\text{Cu}_3(\mu_3\text{-E})]^{3+}$ complexes (E = S and Se) were characterized by resonant X-ray diffraction anomalous fine structure (DAFS), revealing unexpected polarization among the three Cu sites attributed to long-range effects of π -stacking interactions with cocrystallized benzene molecules. The resonant K-edge energies of individual Cu sites within the cluster molecules were found to vary as a function of distance from the cocrystallized benzene. This pattern was interpreted in the context of T-shaped, edge-to-face π -stacking with the assistance of theoretical charge density difference calculations.

The set of forces known as “ π -stacking” interactions are critical to molecular and supramolecular structures in areas ranging from biology and molecular chemistry to materials science.^{1,2} As noncovalent interactions with low binding energies of <5 kcal mol⁻¹, the intimate details of π -stacking are difficult to study experimentally.³ Therefore, although the existence of π -stacking interactions is deduced from experimental structure determination, their detailed electronic structures are typically studied using computational modeling,^{4–6} except in rare cases.^{7–11}

Conveniently, it was recently shown that noncovalent forces can be probed experimentally by analyzing changes in effective nuclear charge (Z_{eff}) of individual metal sites within multinuclear Cu clusters that crystallize in proximity to appropriate guest moieties.^{12,13} The site-specific Z_{eff} trends were probed using X-ray diffraction anomalous fine structure (DAFS) analysis. DAFS is a technique in which single-crystal X-ray diffraction measurements are done at multiple wavelengths below, at, and above the metal K-edge.^{12–22} For a given metal site whose spatial coordinates are well determined in the crystallographic model, the real and imaginary components of anomalous diffraction that contribute to that atom’s scattering factor (eq 1) undergo dramatic changes at that specific site’s resonant energy. Thus, DAFS analysis resolves subtle changes to the K-edge absorption energies of individual metal sites in a metal cluster and, therefore, provides a method by which to probe effects of noncovalent forces acting on the cluster.

$$f = f_0 + f' + if'' \quad (1)$$

A trinucleating, cyclophane-based ligand (abbreviated L herein) developed by one of our groups²³ provides a good venue for isolating remote noncovalent effects on the cluster core from contributions of conformational changes using DAFS, as previously demonstrated for $[\text{LCu}_3(\mu_3\text{-Cl})]^-$.¹² The cluster electronic structures for $\text{LCu}_3(\mu_3\text{-E})$ (E = S and Se) clusters were previously probed using XAS (coupled with DFT

and CASSCF calculations) at the Cu K- and L_{2,3}-edges and the chalcogen K-edges on amorphous samples, collectively indicating near equivalent formal oxidation states for each Cu atom.^{24,25} Here, we have analyzed crystalline samples of $\text{LCu}_3(\mu_3\text{-E})$ (E = S and Se) using DAFS to detect metal site-specific Z_{eff} changes induced by π -stacking interactions with cocrystallized benzene molecules. By comparison to the previously reported XAS results, this study represents a rare case in which the electronic nature of a π -stacking interaction is evidenced experimentally.

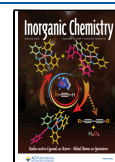
$\text{LCu}_3(\mu_3\text{-S})$ (1) crystallized as a benzene solvate in the C2/c space group with all three Cu sites residing within the asymmetric unit. Although the formal oxidation state assignment for 1 is $1\text{Cu}^1:2\text{Cu}^{\text{II}}$, the coordination geometries and bond distances at the three Cu sites were effectively identical to each other in the crystal structure (Figure 1a) from data obtained at 30 keV. For example, the Cu–S and Cu...Cu distances ranged only from 2.0872(9) Å to 2.0895(8) Å and 3.6098(6) Å to 3.6264(6) Å, respectively. Nonetheless, Cu K-edge DAFS revealed that these three Cu sites are not in electronically equivalent environments (Figure 1b). As in previous Cu K-edge DAFS analyses,^{12,13,17} the dramatic responses seen in the f' vs energy plots for the different Cu sites can be separated into three regions, from lowest energy to highest energy: falling edge, in-edge, and rising edge, with the rising edge region reporting on Z_{eff} .^{12,13,17–19} In this region, the three Cu sites were found to diverge, indicating desymmetrization of Z_{eff} before converging at ~ 9014 eV (assumed to be the

Received: October 25, 2024

Revised: December 3, 2024

Accepted: December 13, 2024

Published: December 16, 2024



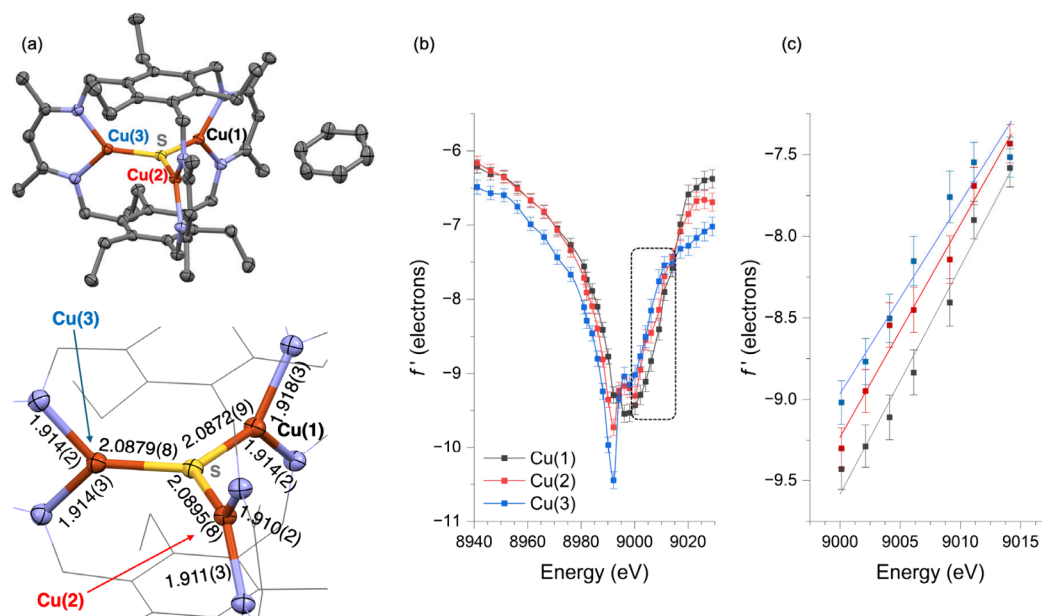


Figure 1. DAFS analysis of $\text{LCu}_3(\mu_3\text{-S})$ (**1**): (a) solid-state structure (50%-probability ellipsoids, hydrogens omitted), with selected bond distances shown in Å; (b) results of f' refinement at different X-ray energies, with the “rising edge” region indicated by a dashed box; (c) linear regression analysis of the rising edge region.

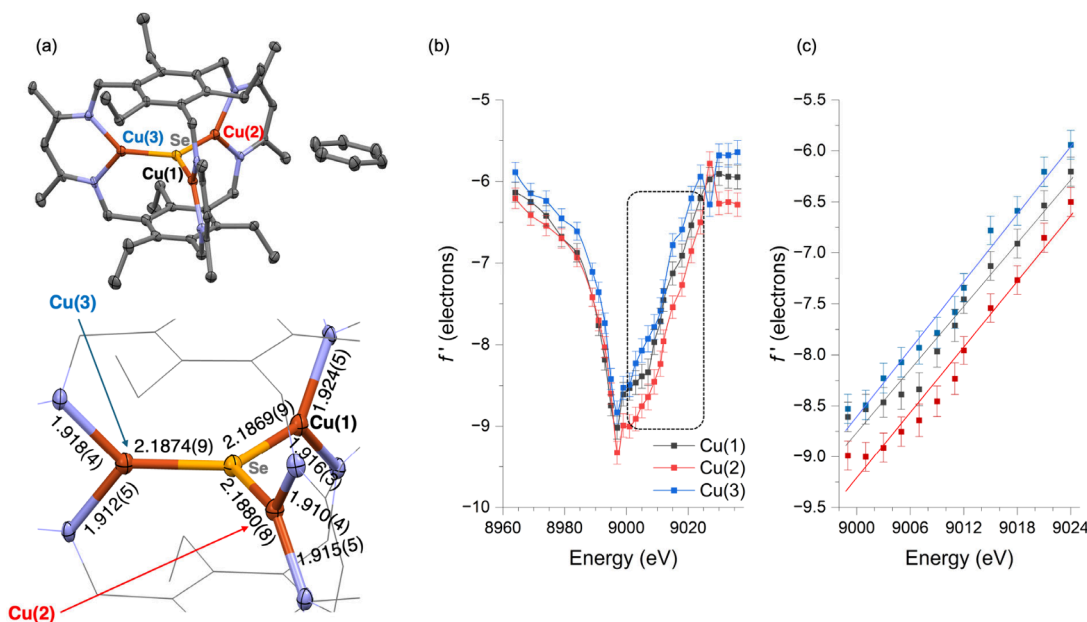


Figure 2. DAFS analysis of $\text{LCu}_3(\mu_3\text{-Se})$ (**2**): (a) solid-state structure (50%-probability ellipsoids, hydrogens omitted), with selected bond distances shown in Å; (b) results of f' refinement at different X-ray energies, with the “rising edge” region indicated by a dashed box; and (c) linear regression analysis of the rising edge region.

white line¹⁸). The Cu(2) and Cu(3) sites track closely with each other along the rising edge, while the Cu(1) rising edge was blue-shifted by ~ 3 eV (Figure 1c). A similar pattern was observed at the rising edge when plotting f'' vs energy (Figure S1). According to the method used in previous Cu K-edge DAFS studies by which the approximately linear portion of the rising edge can be fit by regression,^{12,13,17} we estimate that the rising edge energies of Cu(2) and Cu(3) are within ~ 0.3 eV of each other, while Cu(1) is blue-shifted by ~ 3 eV (Figure 1c). Thus, Cu(1) is assigned as more “oxidized” (i.e., higher Z_{eff}) than Cu(2) and Cu(3), which are more “reduced” to an approximately equal extent. The 3 eV blue shift in rising edge

position is approximately equal in magnitude to the shift assigned to site-specific effects of the K^+ electrostatic field in $[\text{LCu}_3(\mu_3\text{-Cl})]\cdot\text{K}(\text{THF})_3$.¹² In this regard, as discussed further below, it is interesting to note that the Cu(1) site resides closest to the cocrystallized benzene molecule in the crystal lattice (Figure 1a).

$\text{LCu}_3(\mu_3\text{-Se})$ (**2**) also crystallized as a benzene solvate and was found to be isostructural to **1** in $C2/c$. Once again, examination of coordination geometries and bond distances for a structure obtained from 30 keV data did not indicate any metrical dissymmetry within the formally $1\text{Cu}^{\text{I}}:2\text{Cu}^{\text{II}}$ core (Figure 2a). For example, the Cu–Se and Cu \cdots Cu distances

ranged only from 2.1869(9) Å to 2.1880(8) Å and 3.7831(9) Å to 3.7922(9) Å, respectively. Like for **1**, Cu K-edge DAFS data for **2** indicated that the Cu sites reside in different electronic environments (Figure 2b), despite having effectively identical local structures. Importantly, at the rising edge (Figure 2c), the Cu(1) and Cu(3) sites were found to track closely to each other, while the Cu(2) site was found to be blue-shifted by $\sim 6\text{--}7$ eV. A similar rising-edge pattern was observed in the plot of f'' vs energy (Figure S1). Thus, the Cu(2) site is assigned as having the highest Z_{eff} whereas Z_{eff} values for Cu(1) and Cu(3) are lower and clustered together. In other words, the Cu(2) site in **2** is analogous to Cu(1) in **1** and, notably, also sits closest to the cocrystallized benzene molecule in the crystal lattice (Figure 2a).

The rising edge energy of each Cu site is plotted against its distance to the benzene centroid in Figure 3. From this plot, it

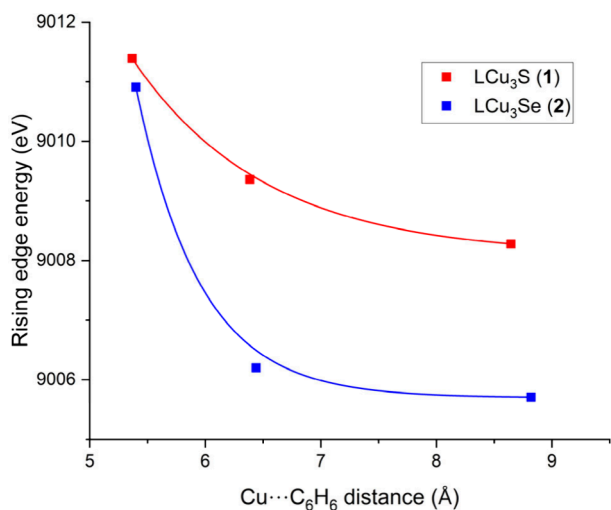


Figure 3. Rising edge energy ($f'' = -8e^-$) as a function of distance from each Cu site to the benzene centroid. Exponential fits are shown only to guide the eye and should not be considered as realistic mathematical models. A corresponding plot of rising edge energy vs centroid-centroid distance is provided in the Supporting Information.

is evident that, for each cluster, there is an approximately exponential decay in Z_{eff} as the Cu centers are displaced further away from the cocrystallized solvent molecule. Furthermore, although we hesitate to realistically fit the decay profiles to mathematical models due to the small number of data points, qualitatively the effect seems to be more dramatic for **2** than for **1**. The shortest Cu \cdots C_{benzene} distances in **1** and **2** are 4.011(4) and 4.018(7) Å, respectively, implying no covalent interaction between any Cu site and the cocrystallized solvents (cf. Cu \cdots C distances of $\sim 2.9\text{--}3.6$ Å for Cu \cdots H–C anagostic interactions).²⁶ Therefore, we hypothesized that noncovalent forces between the cluster and solvent molecules are primarily responsible for the effects evident in Figure 3. In recent studies, we found that counterions or hydrogen bonding interactions with cocrystallized solvent molecules caused polarization among the Cu^I centers of Cu₃(μ_3 -Cl) and Cu₄(μ_4 -S) clusters.^{12,13} We hypothesized that a similar effect operates here, but with some other noncovalent force rather than an electrostatic field or hydrogen bonding effects.

DFT calculations were performed using the coordinates of each asymmetric unit (including cocrystallized benzene molecules) determined by X-ray crystallography. No obvious

differences in Cu charges within a given molecule were evident after examining results from 7 DFT functionals and 5 different charge schemes (i.e., 35 sets of partial atomic charges for each molecule; see Table S2). The situation did not change when allowing the coordinates within the asymmetric unit to optimize or when analyzing the full unit cell using periodic DFT calculations. However, by modeling the LCu(μ_3 -E) compounds with and without the benzene, a pathway for charge transfer became evident by analyzing charge density difference (eq 2).

$$\Delta\rho = \rho_{\text{AB}} - \rho_{\text{A}} - \rho_{\text{B}} \quad (2)$$

The charge density difference for **1** is plotted in Figure 4, and an equivalent plot was derived for **2** and showed very

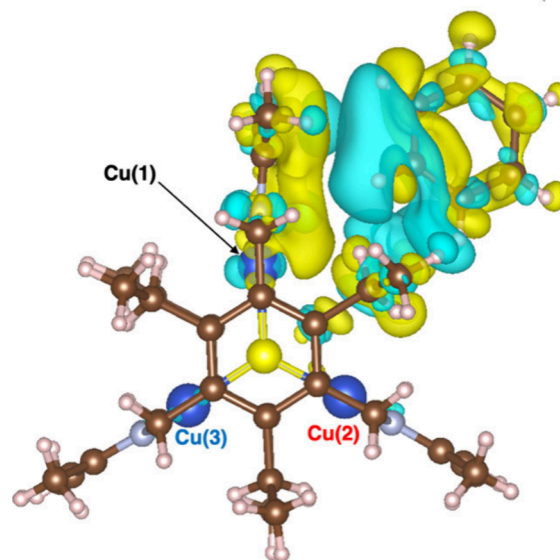


Figure 4. Charge density difference plot for **1** (with and without benzene), 0.0001 e/Bohr³ isosurface, yellow color means a positive density difference (electron accumulation), and blue color means negative density difference (electron depletion).

similar features (Figure S2). Electron accumulation occurs at the β -diketiminato group adjacent to the benzene molecule, while electron depletion occurs at the benzene ring in the region facing the tricopper cluster.

The orientation between the benzene molecule and the 6-membered (β -diketiminato)copper ring with which it interacts resembles a T-shaped π -stacking (edge-to-face) assembly. Such assemblies have been previously proposed based on experimental structure determination and investigated computationally and spectroscopically. For example, in the solid-state, benzene crystallizes in *Pbca* with four molecules in the asymmetric unit, and with each molecule engaging in T-shaped π -stacking interactions with its nearest neighbors.²⁷ The gas-phase experiments of Klemperer and co-workers also indicate the presence of T-shaped benzene dimers,^{28,29} and rotational spectroscopic studies by Arunan and Gutowsky are consistent with the benzene dimer having a T-shaped arrangement with a centroid-to-centroid distance of 4.96 Å in the ground state.³⁰ Computationally, a binding energy of $\sim 2\text{--}3$ kcal mol⁻¹ was determined by Sherrill and co-workers for the T-shaped benzene dimer,³¹ with additional reports demonstrating the role of substituents in stabilizing arene stacking through a combination of dispersion and electrostatic

forces.^{4,32,33} Notably, T-shaped stacks tend to be more favored than other π -stacking motifs when the arene oriented toward the centroid of an unsubstituted benzene is the more-electron-deficient partner (e.g., benzene pointing to the centroid of an electron-rich arene).³⁴ For comparison to the benzene dimer (4.96 Å), the distances between the benzene centroid and the nearest (β -diketiminato)copper centroid in **1** and **2** are 4.726 and 4.776 Å, respectively. In each case, the benzene C–H bond is directed toward the face of the (β -diketiminato)copper unit but canted off center toward the CuN₂ side of the ring rather than aligning with the centroid. Overall, the spatial arrangement suggests that the β -diketimate arm is the more-electron-rich component and the cocrystallized benzene is the more-electron-deficient component of the π -stack, by analogy to Sherrill's calculations. The misalignment of the benzene C–H bond relative to the (β -diketiminato)copper centroid is likely a crystal packing effect, as observed for the solid-state structure of benzene itself.^{1,27}

Based on these results, our working hypothesis is that the T-shaped π -stacking interaction induces the β -diketimate arm near the benzene to be significantly more electron-rich than the other two ligand arms. Furthermore, the DAFS measurements indicate that this dissymmetry in electron density among the ligand arms translates to polarization among the three Cu sites in the cluster molecule. In the absence of π -stacking effects, prior X-ray absorption spectra on amorphous samples of **1** and **2** were best fit using equivalent Cu centers.²⁵ Here, we speculate that the π -stacking interaction induces electron donation from the participating β -diketimate arm toward the benzene ring, resulting in less electron donation to the Cu ion to which it is bound. Then, that Cu ion is less electron-rich, in comparison to the other two Cu sites, an effect that presents as a difference in Z_{eff} in the DAFS experiment. Initially, we anticipated that the greater covalency observed²⁵ for the Cu centers in **2**, relative to **1**, would provide a more-effective means to delocalize the changes arising from the interaction with the benzene. However, the converse is observed—the effect is magnified in **2**, compared to **1** (Figure 3). To probe this effect further, we performed energy decomposition analysis (EDA) of the π -stacking interactions in **1** and **2**. A slightly stronger interaction between benzene and LCu₃(μ_3 -E) was calculated for E = Se (**2**), compared to E = S (**1**). The EDA results (Table S3) revealed that this stronger interaction is primarily from electrostatic contributions, consistent with the fact that Se is more electron-donating than S. Consequently, **2** exhibits a stronger π -stacking interaction with benzene than does **1**, aligned with the findings in Figure 3.

In conclusion, we analyzed Cu site-specific patterns in Z_{eff} for a pair of Cu₃(μ_3 -E) clusters by resonant X-ray diffraction (XRD) techniques. Although one might expect symmetrical distributions of Z_{eff} in these 3-fold-symmetric cluster molecules, charge polarization was evident from the experimental measurements. This polarization was attributed to distal π -stacking interactions between the clusters and cocrystallized benzene molecules. Theoretical charge density difference calculations indicated donation of negative charge from (β -diketiminato)copper groups toward positively charged benzene C–H bonds, in accord with the canonical view of T-shaped π -stacking interactions.

■ ASSOCIATED CONTENT

Supporting Information

The Supporting Information is available free of charge at <https://pubs.acs.org/doi/10.1021/acs.inorgchem.4c04576>.

Methods and additional data (PDF)

Accession Codes

Deposition Nos. 2393901 and 2393902 contain the supplementary crystallographic data for this paper. These data can be obtained free of charge via the joint Cambridge Crystallographic Data Centre (CCDC) and Fachinformationszentrum Karlsruhe [Access Structures](#) service.

■ AUTHOR INFORMATION

Corresponding Authors

Mingjie Liu – Center for Catalysis, Department of Chemistry, University of Florida, Gainesville, Florida 32611, United States; orcid.org/0000-0002-5341-4448; Email: mliu@chem.ufl.edu

Leslie J. Murray – Center for Catalysis and Florida Center for Heterocyclic Chemistry, Department of Chemistry, University of Florida, Gainesville, Florida 32611, United States; orcid.org/0000-0002-1568-958X; Email: murray@chem.ufl.edu

Neal P. Mankad – Department of Chemistry, University of Illinois–Chicago, Chicago, Illinois 60607, United States; orcid.org/0000-0001-6923-5164; Email: npm@uic.edu

Authors

Pinar Alayoglu – Department of Chemistry, University of Illinois–Chicago, Chicago, Illinois 60607, United States

M. Victoria Lorenzo Ocampo – Center for Catalysis, Department of Chemistry, University of Florida, Gainesville, Florida 32611, United States

Zhiyu Wang – Center for Catalysis, Department of Chemistry, University of Florida, Gainesville, Florida 32611, United States

Tieyan Chang – ChemMatCARS, The University of Chicago, Argonne, Illinois 60439, United States; orcid.org/0000-0002-7434-3714

Yu-Sheng Chen – ChemMatCARS, The University of Chicago, Argonne, Illinois 60439, United States

Complete contact information is available at:

<https://pubs.acs.org/doi/10.1021/acs.inorgchem.4c04576>

Author Contributions

The manuscript was written through contributions of all authors. All authors have given approval to the final version of the manuscript.

Notes

The authors declare no competing financial interest.

■ ACKNOWLEDGMENTS

Funding was provided by NIH/NIGMS Grant No. R35 GM140850 (to N.P.M.) and U.S. Department of Energy (DOE) Award (No. DE-SC022174) to L.J.M. NSF's ChemMatCARS, Sector 15 at the Advanced Photon Source (APS), Argonne National Laboratory (ANL) is supported by the Divisions of Chemistry (CHE) and Materials Research (DMR), National Science Foundation, under Grant No. NSF/CHE-1834750. This research used resources of the APS, a DOE Office of Science user facility operated by ANL, under

Contract No. DE-AC02-06CH11357. M.L. acknowledges the University of Florida Research Computing for providing computational resources and support.

REFERENCES

- (1) Meyer, E. A.; Castellano, R. K.; Diederich, F. Interactions with Aromatic Rings in Chemical and Biological Recognition. *Angew. Chem., Int. Ed.* **2003**, *42* (11), 1210–1250.
- (2) Martinez, C. R.; Iverson, B. L. Rethinking the Term “Pi-Stacking”. *Chem. Sci.* **2012**, *3* (7), 2191–2201.
- (3) Müller-Dethlefs, K.; Hobza, P. Noncovalent Interactions: A Challenge for Experiment and Theory. *Chem. Rev.* **2000**, *100* (1), 143–168.
- (4) Sherrill, C. D. Energy Component Analysis of π Interactions. *Acc. Chem. Res.* **2013**, *46* (4), 1020–1028.
- (5) Wheeler, S. E. Understanding Substituent Effects in Noncovalent Interactions Involving Aromatic Rings. *Acc. Chem. Res.* **2013**, *46* (4), 1029–1038.
- (6) Carter-Fenk, K.; Herbert, J. M. Reinterpreting π -Stacking. *Phys. Chem. Chem. Phys.* **2020**, *22* (43), 24870–24886.
- (7) Cockroft, S. L.; Hunter, C. A.; Lawson, K. R.; Perkins, J.; Urch, C. J. Electrostatic Control of Aromatic Stacking Interactions. *J. Am. Chem. Soc.* **2005**, *127* (24), 8594–8595.
- (8) Hunter, C. A.; Low, C. M. R.; Vinter, J. G.; Zonta, C. Quantification of Functional Group Interactions in Transition States. *J. Am. Chem. Soc.* **2003**, *125* (33), 9936–9937.
- (9) Rashkin, M. J.; Waters, M. L. Unexpected Substituent Effects in Offset Π - π Stacked Interactions in Water. *J. Am. Chem. Soc.* **2002**, *124* (9), 1860–1861.
- (10) Kim, E.; Paliwal, S.; Wilcox, C. S. Measurements of Molecular Electrostatic Field Effects in Edge-to-Face Aromatic Interactions and CH- π Interactions with Implications for Protein Folding and Molecular Recognition. *J. Am. Chem. Soc.* **1998**, *120* (43), 11192–11193.
- (11) Paliwal, S.; Geib, S.; Wilcox, C. S. Molecular Torsion Balance for Weak Molecular Recognition Forces. Effects of “Tilted-T” Edge-to-Face Aromatic Interactions on Conformational Selection and Solid-State Structure. *J. Am. Chem. Soc.* **1994**, *116* (10), 4497–4498.
- (12) Alayoglu, P.; Chang, T.; Lorenzo Ocampo, M. V.; Murray, L. J.; Chen, Y.-S.; Mankad, N. P. Metal Site-Specific Electrostatic Field Effects on a Tricopper(I) Cluster Probed by Resonant Diffraction Anomalous Fine Structure (DAFS). *Inorg. Chem.* **2023**, *62* (37), 15267–15276.
- (13) Alayoglu, P.; Rathnayaka, S.; Chang, T.; Wang, S. G.; Chen, Y.-S.; Mankad, N. Cu Site Differentiation in Tetracopper(I) Sulfide Clusters Enables Biomimetic N₂O Reduction. *Chem. Sci.* **2024**, *15*, 13668–13675.
- (14) Einsle, O.; Andrade, S. L. A.; Dobbek, H.; Meyer, J.; Rees, D. C. Assignment of Individual Metal Redox States in a Metalloprotein by Crystallographic Refinement at Multiple X-Ray Wavelengths. *J. Am. Chem. Soc.* **2007**, *129* (8), 2210–2211.
- (15) Spatzal, T.; Schlesier, J.; Burger, E.-M.; Sippel, D.; Zhang, L.; Andrade, S. L. A.; Rees, D. C.; Einsle, O. Nitrogenase FeMoco Investigated by Spatially Resolved Anomalous Dispersion Refinement. *Nat. Commun.* **2016**, *7* (1), 10902.
- (16) Zhang, L.; Kaiser, J. T.; Meloni, G.; Yang, K. Y.; Spatzal, T.; Andrade, S. L. A.; Einsle, O.; Howard, J. B.; Rees, D. C. The Sixteenth Iron in the Nitrogenase MoFe Protein. *Angew. Chem. - Int. Ed.* **2013**, *52* (40), 10529–10532.
- (17) Alayoglu, P.; Chang, T.; Yan, C.; Chen, Y.-S.; Mankad, N. Uncovering a CF₃ Effect on X-Ray Absorption Energies of [Cu(CF₃)₄]⁻ and Related Cu Compounds Using Resonant Diffraction Anomalous Fine Structure (DAFS) Measurements. *Angew. Chem., Int. Ed.* **2023**, *62* (51), No. e202313744.
- (18) Bartholomew, A. K.; Teesdale, J. J.; Hernandez Sanchez, R.; Malbrecht, B. J.; Juda, C. E.; Menard, G.; Bu, W.; Iovan, D. A.; Mikhailina, A. A.; Zheng, S.-L.; et al. Exposing the Inadequacy of Redox Formalisms by Resolving Redox Inequivalence within Isovalent Clusters. *Proc. Natl. Acad. Sci. U. S. A.* **2019**, *116* (32), 15836–15841.
- (19) Bartholomew, A. K.; Musgrave, R. A.; Anderton, K. J.; Juda, C. E.; Dong, Y.; Bu, W.; Wang, S.-Y.; Chen, Y.-S.; Betley, T. A. Revealing Redox Isomerism in Trichromium Imides by Anomalous Diffraction. *Chem. Sci.* **2021**, *12*, 15739–15749.
- (20) Gao, Y.; Frost-Jensen, A.; Pressprich, M. R.; Coppens, P.; Marquez, A.; Dupuis, M. Valence Contrast by Synchrotron Resonance Scattering: Application to a Mixed-Valence Manganese Compound. *J. Am. Chem. Soc.* **1992**, *114* (23), 9214–9215.
- (21) Gao, Y.; Pressprich, M. R.; Coppens, P. Anomalous-scattering Contrast Study of the Mixed-valence Charge-density-wave Conductor NbSe₃. *Acta Crystallogr., Sect. A* **1993**, *49* (1), 216–219.
- (22) Hernández Sánchez, R.; Champsaur, A. M.; Choi, B.; Wang, S. G.; Bu, W.; Roy, X.; Chen, Y. S.; Steigerwald, M. L.; Nuckolls, C.; Paley, D. W. Electron Cartography in Clusters. *Angew. Chem. - Int. Ed.* **2018**, *57* (42), 13815–13820.
- (23) Ferreira, R. B.; Murray, L. J. Cyclophanes as Platforms for Reactive Multimetallic Complexes. *Acc. Chem. Res.* **2019**, *52* (2), 447–455.
- (24) Di Francesco, G. N.; Gaillard, A.; Ghiviriga, I.; Abboud, K. A.; Murray, L. J. Modeling Biological Copper Clusters: Synthesis of a Tricopper Complex, and Its Chloride- and Sulfide-Bridged Congeners. *Inorg. Chem.* **2014**, *53* (9), 4647–4654.
- (25) Cook, B. J.; Di Francesco, G. N.; Ferreira, R. B.; Lukens, J. T.; Silberstein, K. E.; Keegan, B. C.; Catalano, V. J.; Lancaster, K. M.; Shearer, J.; Murray, L. J. Chalcogen Impact on Covalency within Molecular [Cu₃(M3-E)]³⁺ Clusters (E = O, S, Se): A Synthetic, Spectroscopic, and Computational Study. *Inorg. Chem.* **2018**, *57* (18), 11382–11392.
- (26) dos Passos Gomes, G.; Xu, G.; Zhu, X.; Chamoreau, L. M.; Zhang, Y.; Bistri-Aslanoff, O.; Roland, S.; Alabugin, I. V.; Sollogoub, M. Mapping C–H...M Interactions in Confined Spaces: (α -ICyDMe)Au, Ag, Cu Complexes Reveal “Contra-Electrostatic H Bonds” Masquerading as Anagostic Interactions**. *Chem. - Eur. J.* **2021**, *27* (31), 8127–8142.
- (27) Cox, E. G.; Cruickshank, D. W. J.; Smith, J. A. S. The Crystal Structure of Benzene at -3° C. *Proc. R. Soc. London Ser. Math. Phys. Sci.* **1958**, *247* (1248), 1–21.
- (28) Janda, K. C.; Hemminger, J. C.; Winn, J. S.; Novick, S. E.; Harris, S. J.; Klemperer, W. Benzene Dimer: A Polar Molecule. *J. Chem. Phys.* **1975**, *63* (4), 1419–1421.
- (29) Steed, J. M.; Dixon, T. A.; Klemperer, W. Molecular Beam Studies of Benzene Dimer, Hexafluorobenzene Dimer, and Benzene–Hexafluorobenzene. *J. Chem. Phys.* **1979**, *70* (11), 4940–4946.
- (30) Arunan, E.; Gutowsky, H. S. The Rotational Spectrum, Structure and Dynamics of a Benzene Dimer. *J. Chem. Phys.* **1993**, *98* (5), 4294–4296.
- (31) Sinnokrot, M. O.; Valeev, E. F.; Sherrill, C. D. Estimates of the Ab Initio Limit for Π - π Interactions: The Benzene Dimer. *J. Am. Chem. Soc.* **2002**, *124* (36), 10887–10893.
- (32) Sinnokrot, M. O.; Sherrill, C. D. High-Accuracy Quantum Mechanical Studies of Π - π Interactions in Benzene Dimers. *J. Phys. Chem. A* **2006**, *110* (37), 10656–10668.
- (33) Sinnokrot, M. O.; Sherrill, C. D. Highly Accurate Coupled Cluster Potential Energy Curves for the Benzene Dimer: Sandwich, T-Shaped, and Parallel-Displaced Configurations. *J. Phys. Chem. A* **2004**, *108* (46), 10200–10207.
- (34) Hunter, C. A.; Sanders, J. K. M. The Nature of π - π Interactions. *J. Am. Chem. Soc.* **1990**, *112* (14), 5525–5534.